size in which the rate of molecular motion is sufficiently fast to maintain thermal equilibrium at all times; the normalization constant for the Boltzmann distribution is $p_0 = 1/(\lambda\pi^{1/2})$ for x on $(-\infty,+\infty)$. The concentration of reduced molecules B at point x at time t is given by an expression analogous to eq 25, which when integrated over all x_0, with $b(x_0,t)$ expanded as a Taylor series about $x = x_0$, yields

$$C_B(x,t) = C_E\int_{-\infty}^{+\infty} b(x_0,t)\, p(x,x_0)\, dx_0 = C_E\sum_{n=0}^{\infty}\frac{1}{n!}\left(\frac{\lambda}{2}\right)^{2n}\left(\frac{\partial^{2n}b(x,t)}{\partial x^{2n}}\right)_x \approx C_E b(x,t) \quad (28)$$

Note that the function $b(x,x_0)$ defined in the preceding section is independent of the molecule's position for a system of infinite size but does dependent upon time for non-steady-state conditions; hence we write $b(x_0,t)$ instead of $b(x,x_0)$. Truncation of eq 28 after the first term introduces negligible error so long as the thickness of the diffusion layer is much larger than λ. Therefore, Fick's second law

$$\frac{\partial C_B(x,t)}{\partial t} = D_{ap}\frac{\partial^2 C_B(x,t)}{\partial x^2}$$

is completely equivalent to

$$\frac{\partial b(x,t)}{\partial t} = D_{ap}\frac{\partial^2 b(x,t)}{\partial x^2} \quad (29)$$

Because the molecules are always at thermal equilibrium within the potential energy well, there is no net transport of charge arising from physical motion. The time dependence of $b(x,t)$ arises exclusively from electron hopping; hence we apply the standard rate laws to evaluate the rate of change in $b(x,t)$ arising from electron exchange reactions. To account for all electron-transfer reactions affecting $b(x_0,t)$, we must locate all molecules possessing fixed point x_0, their current positions being x, and all molecules of the opposite oxidation state within a distance δ of x, such molecules having fixed points at $\hat{x}_0$. The rate constant for electron exchange between two *specific* molecules is k_{act} divided by the reaction surface "area" (recall that k_{act} applies to electron transfer to *any* site within the reaction distance δ). In one dimension this quantity is $k_{act}/2$, in two dimensions $k_{act}/(2\pi\delta)$, and in three dimensions $k_{act}/(4\pi\delta^2)$. The resulting master kinetic equation in one dimension is

$$\frac{\partial b(x_0,t)}{\partial t} = \frac{k_{act}C_E}{2\lambda^2\pi}\int_{-\infty}^{+\infty}\int_{-\infty}^{+\infty}(b(\hat{x}_0,t) - b(x_0,t))p(x,x_0) \times (p(x-\delta,\hat{x}_0) + p(x+\delta,\hat{x}_0))\, dx\, d\hat{x}_0$$

Expansion of $b(\hat{x}_0,t)$ as a Taylor series about x_0 followed by integration over $\hat{x}_0$ and x, using binomial series expansions where necessary, yields

$$\frac{\partial b(x_0,t)}{\partial t} = k_{act}C_E\sum_{n=1}^{\infty}\left(\frac{\partial^{2n}b(x,t)}{\partial x^{2n}}\right)_{x_0}\sum_{m=0}^{n}\sum_{k=m}^{n}\frac{(\lambda/2)^{2k}\delta^{2n-2k}}{(k-m)!\,(2n-2k)!} \quad (30)$$

The derivations in two and three dimensions are completely analogous to that shown above, except that the reaction surface is a circle in two dimensions and a sphere in three dimensions; the exact expressions for $\partial b(x_0,t)/\partial t$ in two and three dimensions are, of course, slightly different than that of eq 30. Provided the diffusion layer is much larger than λ, only the first term in the series expansion for $\partial b(x_0,t)/\partial t$ is significant. On the basis of the derivations for $\nu = 1$, 2, and 3, with terms for $n \geq 2$ discarded, a general equation is obtained

$$\frac{\partial b(x_0,t)}{\partial t} = \frac{1}{2\nu}k_{act}C_E(\delta^2 + \nu\lambda^2)\left(\frac{\partial^2 b(x,t)}{\partial x^2}\right)_{x_0}$$

which is identical to eq 29 with D_{ap} given by eqs 20 and 22 (written using $k_{act}C_E$ instead of X/t_e).

Identification of the Iron Ions of High Potential Iron Protein from *Chromatium vinosum* within the Protein Frame through Two-Dimensional NMR Experiments

Ivano Bertini,*,† Francesco Capozzi,‡ Stefano Ciurli,‡ Claudio Luchinat,‡ Luigi Messori,† and Mario Piccioli†

Contribution from the Department of Chemistry, University of Florence, Florence, Italy, and the Institute of Agricultural Chemistry, University of Bologna, Bologna, Italy.
Received August 26, 1991

Abstract: 2D NMR experiments performed on both the oxidized and reduced form of the high potential iron protein (HiPIP) from *Chromatium vinosum*, a paramagnetic iron sulfur protein for which the crystal structure is known in both oxidation states, allowed us to detect a number of scalar and dipolar connectivities of the isotropically shifted signals. On this basis it was possible to firmly identify the signals of the β-CH_2 and α-CH protons of the cluster-liganded cysteines and perform their sequence-specific assignments. The assignments mainly rely on the observation of NOESY cross peaks from β or α Cys protons to protons assigned to the few aromatic residues surrounding the cluster. This is the first sequence-specific assignment of Cys β-CH_2 protons for a Fe_4S_4 cluster. In the light of existing experimental evidence from Mössbauer data and of the theoretical model describing the magnetic coupling of the metal centers in the oxidized form, the present assignment establishes which iron ions of the oxidized cluster are in a pure ferric state and which are in a mixed valence state. These findings may be relevant as far as the actual mechanism of electron transfer is concerned. In addition, information is obtained on the angular dependence of the β-CH_2 hyperfine shifts in iron sulfur systems.

Introduction

The understanding of the functional properties of iron–sulfur proteins[1] stands on the knowledge of the electronic structure of the clusters and on the location of the various types of iron ions within the protein frame. Progress in the knowledge of the electronic structure of iron–sulfur clusters is due to a variety of

† University of Florence.
‡ University of Bologna.

(1) (a) Lovenberg, W., Ed. *Iron Sulfur Proteins*; Academic Press: New York, 1973, Vol. 1, 2; 1977, Vol. 3. (b) Spiro, T. G., Ed. *Metal Ions in Biology*; Wiley-Interscience: New York, 1982; Vol. 4. (c) Sweeney, W. V.; Rabinowitz, J. C. *Annu. Rev. Biochem.* **1980**, *49*, 139.

0002-7863/92/1514-3332$03.00/0

investigation tools. Because of the one-electron carrier function of iron–sulfur proteins in biological processes, the clusters contain iron in various oxidation states, thus making Mössbauer spectroscopy a valid means to characterize the iron ions in the cluster core. Information on the hyperfine coupling between the ^{57}Fe nuclei or the proton nuclei around the cluster, and the electron spin magnetic moment located on each iron, is provided, respectively, by magnetic Mössbauer and ^1H NMR spectroscopy. By using the signs of the hyperfine coupling constants derived from Mössbauer spectroscopy for each iron oxidation state, NMR can provide a more detailed picture of the protein environment around the cluster, thus allowing the assignment of the oxidation states to each iron ion, because of the amplification of differences among the four subsites due to the hyperfine contribution to the chemical shifts.[2] Theoretical models have also been developed to account for the electronic structure.[3-17]

In the case of reduced [2Fe–2S] proteins, containing the $[Fe_2S_2]^+$ core, Mössbauer and EPR data have shown that the protein contains one iron(II) and one iron(III) to give total spin $S = {}^1/_2$.[18,19] ^1H NMR spectra have shown that only one specific iron within the protein is reduced;[20] the details of the proton hyperfine coupling have been understood[9,21] and the identity of the reduced iron ion in the protein has been ascertained.[22]

In the case of reduced [3Fe–4S] proteins, containing the $[Fe_3S_4]^0$ cluster, formally two iron(III) and one iron(II) are present. The $S = 2$ ground state has been proposed on the basis of MCD studies.[23] Mössbauer spectroscopy has shown the presence of one iron(III) and of a mixed valence pair constituted by the iron(II) and one iron(III) to give an oxidation state of +2.5.[6,24,25] A theoretical model has been developed, which shows that the $S = 2$ ground state can result from antiferromagnetic coupling between an $S = {}^9/_2$ state of the mixed valence pair and an $S = {}^5/_2$ state of the third iron ion.[6] The approach required the introduction of a double exchange operator which accounts for the delocalization of one electron within the mixed valence pair. It has also been argued that the use of different J values in the simple Heisenberg approach provides the same ground state and a similar pattern of low lying excited states.[10] It appears therefore that there is large covariance between the introduction of the double exchange operator on an iron(III)–iron(II) pair and a reduction in the value of the J constant in the Heisenberg exchange operator for the same pair.

Oxidized high potential iron–sulfur proteins (HiPIPs) are examples of [4Fe–4S] clusters which contain three iron(III) and one iron(II). These proteins have been studied by a variety of spectroscopic techniques, such as Mössbauer,[26,27] electron paramagnetic resonance,[28,29] electron nuclear double resonance,[30] magnetic circular dichroism,[31] resonance Raman,[32] and NMR[10,13-16,33-38] spectroscopy. Mössbauer data on HiPIP from *C. vinosum* show that indeed the cluster contains two Fe^{3+} and two $Fe^{2.5+}$ ions.[26,27] The hyperfine coupling with ^{57}Fe shows that the mixed valence pair has a larger ground-state S value than that of the ferric pair.[27] It is likely that the two subspin states are $S = {}^9/_2$ and $S = 4$, respectively,[5] although other combinations giving total $S = {}^1/_2$, such as $S = {}^7/_2$ and $S = 3$, are also conceivable.[15,39]

The ^1H NMR spectra of oxidized HiPIPs from *C. vinosum*,[13] *E. halophila*,[14] and *R. gelatinosa*[15] show two sets of different sign of the hyperfine coupling between the unpaired electrons on each iron ion and the β-CH_2 protons of cysteines bound to the cluster. This is consistent with an antiferromagnetic coupling between the larger and the smaller spin. The nuclei coupled with the larger spin experience a negative induced electron magnetic moment $\langle S_z \rangle$. A negative $\langle S_z \rangle$ is the normal situation for isolated 3d metal ions. On the other hand, the nuclei coupled with the smaller spin experience a positive $\langle S_z \rangle$ value. The latter behavior always holds at low temperature, where no excited states are appreciably populated, but at room temperature the excited states must be taken into account.[13]

A theoretical approach has rationalized these findings in terms of a Heisenberg exchange operator on the ferric pair having a larger exchange coupling than all the others plus a double exchange operator on the iron(III)–iron(II) pair.[5,13,15] As in the trimetallic cluster,[10] analogous results are again obtained by using one exchange coupling constant larger than the others on the ferric ions, and one smaller than the others on the iron(III)–iron(II) pair, without a double exchange operator.[13-15] These findings show that a reliable estimate of the double exchange constant cannot be obtained from the above data only, but independent information is needed.[8]

We have now developed the necessary technology to detect connectivities in 2D ^1H NMR spectra of fast relaxing nuclei, with the aim of performing sequence-specific assignments of the cysteine protons. In this way we will establish which cysteines are coupled

(2) Bertini, I.; Luchinat, C. *NMR of Paramagnetic Molecules in Biological Systems*; Benjamin Cummings: Menlo Park, CA, 1986.
(3) Girerd, J.-J. *J. Chem. Phys.* **1983**, *79*, 1776.
(4) Papaefthymiou, V.; Girerd, J.-J.; Moura, I.; Moura, J. J. G.; Munck, E. *J. Am. Chem. Soc.* **1987**, *109*, 4703.
(5) Noodleman, L. *Inorg. Chem.* **1988**, *27*, 3677.
(6) Munck, E.; Papaefthymiou, V.; Sererus, K. K.; Girerd, J.-J. In *Metal Clusters in Proteins*; ACS Symposium Series; Que, L., Ed.; American Chemical Society: Washington, DC, 1988.
(7) Borshch, S. A.; Chibotaru, L. F. *Chem. Phys.* **1989**, *135*, 375.
(8) Blondin, G.; Girerd, J.-J. *Chem. Rev.* **1990**, *90*, 1359.
(9) Banci, L.; Bertini, I.; Luchinat, C. *Struct. Bonding* **1990**, *72*, 113.
(10) Bertini, I.; Briganti, F.; Luchinat, C. *Inorg. Chim. Acta* **1990**, *175*, 9.
(11) Barbaro, P.; Bencini, A.; Bertini, I.; Briganti, F.; Midollini, S. *J. Am. Chem. Soc.* **1990**, *112*, 7238.
(12) Noodleman, L. *Inorg. Chem.* **1991**, *30*, 246.
(13) Bertini, I.; Briganti, F.; Luchinat, C.; Scozzafava, A.; Sola, M. *J. Am. Chem. Soc.* **1991**, *113*, 1237.
(14) Banci, L.; Bertini, I.; Briganti, F.; Luchinat, C.; Scozzafava, A.; Vicens Oliver, M. *Inorg. Chim. Acta* **1991**, *180*, 171.
(15) Banci, L.; Bertini, I.; Briganti, F.; Luchinat, C.; Scozzafava, A.; Vicens Oliver, M. *Inorg. Chem.* **1991**, *30*, 4517.
(16) Banci, L.; Bertini, I.; Briganti, F.; Luchinat, C. *New J. Chem.* **1991**, *15*, 467.
(17) Bertini, I.; Briganti, F.; Luchinat, C.; Messori, L.; Monnanni, R.; Scozzafava, A.; Vallini, G. *Eur. J. Biochem.*, in press.
(18) Fee, J. A.; Findling, K. L.; Yoshida, T.; Hill, R.; Tarr, G. E.; Hearshen, D. O.; Dunham, W. R.; Day, E. P.; Kent, T. A.; Munck, E. *J. Biol. Chem.* **1984**, *259*, 124.
(19) Gibson, J. F.; Hall, D. O.; Thornley, J. H. M.; Whatley, F. R. *Proc. Natl. Acad. Sci. U.S.A.* **1966**, *56*, 987.
(20) Bertini, I.; Lanini, G.; Luchinat, C. *Inorg. Chem.* **1984**, *23*, 2729.
(21) Dunham, W. R.; Palmer, G.; Sands, R. H.; Bearden, A. J. *Biochim. Biophys. Acta* **1971**, *253*, 373.
(22) Dugad, L. B.; La Mar, G. N.; Banci, L.; Bertini, I. *Biochemistry* **1990**, *29*, 2263.
(23) Thomson, A. J.; Robinson, A. E.; Johnson, M. K.; Moura, J. J. G.; Moura, I.; Xavier, A.; LeGall, J. *Biochim. Biophys. Acta* **1981**, *670*, 93.
(24) Huynh, B. H.; Moura, J. J. G.; Moura, I.; Kent, T. A.; LeGall, J.; Xavier, A.; Munck, E. *J. Biol. Chem.* **1980**, *255*, 3242.
(25) Moura, J. J. G.; Moura, I.; Kent, T. A.; Lipscomb, J. D.; Huynh, B. H.; LeGall, J.; Xavier, A.; Munck, E. *J. Biol. Chem.* **1982**, *257*, 6259.
(26) Dickson, D. P. E.; Johnson, C. E.; Cammack, R.; Evans, M. C. W.; Hall, D. O.; Rao, K. K. *Biochem. J.* **1974**, *139*, 105.
(27) Middleton, P.; Dickson, D. P. E.; Johnson, C. E.; Rush, J. D. *Eur. J. Biochem.* **1980**, *104*, 289.
(28) Antanaitis, B. C.; Moss, T. H. *Biochim. Biophys. Acta* **1975**, *405*, 262.
(29) Peisach, J.; Orme-Johnson, N. R.; Mims, W. B.; Orme-Johnson, W. H. *J. Biol. Chem.* **1977**, *252*, 5643.
(30) Anderson, R. E.; Anger, G.; Petersson, L.; Ehrenberg, A.; Cammack, R.; Hall, D. O.; Mullinger, R.; Rao, K. K. *Biochim. Biophys. Acta* **1975**, *376*, 63.
(31) Johnson, M. K.; Thomson, A. J.; Robinson, A. E.; Rao, K. K.; Hall, D. O. *Biochim. Biophys. Acta* **1981**, *667*, 433.
(32) Backes, G.; Mino, Y.; Loehr, T. M.; Meyer, T. E.; Cusanovich, M. A.; Sweeney, W. V.; Adman, E. T.; Sanders-Loehr, J. *J. Am. Chem. Soc.* **1991**, *113*, 2055.
(33) Phillips, W. B.; Poe, M.; McDonald, C. C.; Bartsch, R. G. *Proc. Natl. Acad. Sci. U.S.A.* **1970**, *67*, 682.
(34) Nettesheim, D. G.; Meyer, T. E.; Feinberg, B. A.; Otvos, J. D. *J. Biol. Chem.* **1983**, *258*, 8235.
(35) Krishnamoorthi, R.; Markley, J. R.; Cusanovich, M. A.; Prysiecki, C. T.; Meyer, T. E. *Biochemistry* **1986**, *25*, 60.
(36) Krishnamoorthi, R.; Cusanovich, M. A.; Meyer, T. E.; Prysiecki, C. T. *Eur. J. Biochem.* **1989**, *181*, 81.
(37) Sola, M.; Cowan, J. A.; Gray, H. B. *Biochemistry* **1989**, *28*, 5261.
(38) Cowan, J. A.; Sola, M. *Biochemistry* **1990**, *29*, 5633.
(39) Mouesca, J. M.; Lamotte, B.; Rius, G. J. *Inorg. Biochem.* **1991**, *43*, 251.

to the ferric ions and which are coupled to the iron(III)–iron(II) pair. This allows us to have a complete picture of the surroundings of the Fe_4S_4 cluster and, by comparison with the available X-ray structure, to have information on the unpaired electron delocalization mechanism from iron to proton. The resulting picture is important to understand the biological role of the electron transfer proteins.

Experimental Section

All chemicals used were of the best quality available. Reduced HiPIP was isolated from *C. vinosum* according to the procedures reported by Bartsch.[40] Protein purity was checked by UV–vis spectroscopy.

Sample deuteration was performed by solvent exchange utilizing an ultrafiltration Amicon cell, equipped with a YM1 membrane. At least five changes of deuterated buffer were performed to ensure satisfactory solvent exchange. Protein samples were oxidized by addition of stoichiometric amounts of sodium ferricyanide; the extent of oxidation was checked by measuring the area of the NMR peaks corresponding to the various redox species.

All NMR data have been collected on samples dissolved in D_2O solutions, 50 mM phosphate buffer. Reduced protein samples were at pH* 7.2, and oxidized protein samples were at pH* 5.4. Mixtures of reduced and oxidized protein for EXSY experiments were at pH* 5.3.

All the ^1H NMR spectra were recorded on an AMX Bruker spectrometer operating at 600 MHz Proton Larmor Frequency; unless otherwise specified temperature was always 300 K. The 300 K spectra were calibrated against the residual HDO signal, and the latter assigned a shift of 4.80 ppm with respect to DSS.

1D nuclear Overhauser effect (NOE) difference spectra have been collected using previously reported methodology.[41] T_1 values were measured using the inversion recovery method.

2D COSY spectra were recorded in the magnitude mode.[42,43] Spectra were recorded with 128–1024 t_1 values and 200–2000 scans per t_1 value, 1K in f_2. Repetition times were 60–300 ms. Prior to Fourier transformation, the 2D data matrix was multiplied by an unshifted squared sine bell window function in both dimensions, unless otherwise specified.

2D NOESY spectra were recorded in the phase sensitive mode, with the sequence RD–90–t_1–90–t_m–90–AQ.[44] Spectra were recorded with 256–512 t_1 values and 500–2000 scans per t_1 value, 1K data points in f_2. Repetition times were 120–500 ms. Several experiments were performed with mixing times of 5, 10, or 18 ms. Prior to Fourier transformation, the data matrix was multiplied by a phase-shifted squared sine bell window function in both dimensions.

2D TOCSY spectra were acquired with the RD–90–t_1–SL–MLEV 17–SL–AQ pulse sequence, where SL denotes a short spin lock field applied along the x axis and MLEV 17 is a composite pulse sequence.[45] The repetition time was 400 ms; mixing times of 10, 20 and 40 ms were used. Prior to Fourier transformation, the data matrix was multiplied by a squared cosine bell window function in both dimensions.

The 2D saturation transfer experiment (EXSY) was recorded in the phase sensitive mode with the standard phase sensitive NOESY sequence, using a mixing time of 15 ms.[46] The spectrum was recorded with 512 t_1 values and 128 scans per t_1 value, 1K data points in f_2. The repetition time was 500 ms.

In order to improve detection of isotropically shifted signals, in some of the 2D experiments we used a low power MLEV 16 pulse sequence in front of the 2D sequence to presaturate the diamagnetic part of the spectrum.

A standard Bruker software package was used for data processing.

Results

Pairwise Assignment of β-CH_2 Protons in Reduced and Oxidized Forms. A schematic drawing of the metal cluster and of the coordinated cysteines is shown in Figure 1.

In a previous work the signals corresponding to the β-CH_2 protons of the metal liganded cysteines had been identified and pairwise connected through 1D NOE experiments in both the reduced and oxidized form.[13] Saturation transfer experiments allowed correlation of the isotropically shifted signals in the two redox species.[13] We used these results as a starting point for the specific assignment of the metal coordinated cysteines.

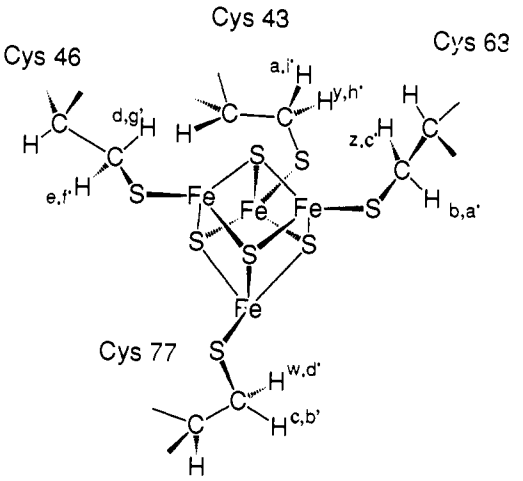

Figure 1. Schematic drawing of the metal cluster of *C. vinosum* HiPIP. Cys β-CH_2 protons are labeled according to their assignment in the ^1H NMR spectra of the reduced and oxidized protein (see Figure 2) as shown in the present work.

Correspondences between the signals in the oxidized and reduced forms are summarized in Figure 2 for ease of reference. The established correspondences are between the following signals: a–i′ and y–h′ for cysteine I, d–g′ and e–f′ for cysteine II, b–a′ and z–c′ for cysteine III, and c–b′ and w–d′ for cysteine IV, where numbers I to IV are arbitrarily assigned to the four coordinated cysteines. The primes indicate the oxidized protein.

Scalar and Dipolar Connectivities within the Cluster Ligands. We have proceeded in the search for scalar connectivities, with the aim of further checking the correctness of the assignment of Cys β-CH_2 signals and of identifying as many β-CH_2/α-CH connectivities as possible. The magnitude COSY spectra of the reduced and oxidized proteins are reported in Figures 3A and 4, respectively.

In the reduced protein, COSY cross peaks are apparent for the following signals (Figure 3A): signal a gives a COSY cross peak with signal y, signal b with signal z and a signal at 3.75 ppm, signal c with signal w and a signal at 8.52 ppm, and signal d with signal e and a signal at 4.3 ppm. No other COSY cross peaks are detected for signal e.

In the oxidized protein (Figure 4), COSY cross peaks are detected between signals b′ and d′ and h′ and i′ (signal a′ was intentionally left out of the spectral window to improve resolution). The inability to observe COSY cross peaks between f′ and g′ in the oxidized form is due to the proximity of the two signals, which is maintained over the accessible temperature range.

The above experiments, taken together, confirm the assignment of the geminal β-CH_2 pairs of all cysteines, and allow the firm identification of the α-CH proton signals of cysteines II, III, and IV in the reduced form (signals at 4.3, 3.75, and 8.52 ppm, respectively). Saturation transfer between signal e′ and the signal at 8.52 ppm (signal v) had already been observed;[13] this permits the firm assignment of signal e′ as the α-CH proton of Cys IV as anticipated on the basis of the observed NOEs between e′ and both b′ and d′.[13]

As far as dipolar connectivities are concerned, the NOESY spectrum of the reduced protein is shown in Figure 3B; for the oxidized protein 1D NOEs are reported in Figure 5. Below we describe the strategy that we have utilized to analyze the many dipolar connectivities observed in these spectra in order to achieve a sequence-specific assignment of the cluster-coordinated cysteines.

Strategy for Sequence-Specific Assignments. The strategy that we report here to obtain sequence-specific assignments of the cluster-coordinated cysteines starts from the observation that in the crystal structure of oxidized *C. vinosum* HiPIP[47] some Cys

(40) Bartsch, R. G. *Methods Enzymol.* **1978**, *53*, 329.
(41) (a) Lecomte, J. T. J.; Unger, S. W.; LaMar, G. N. *J. Magn. Reson.* **1991**, *94*, 112. (b) Banci, L.; Bertini, I.; Luchinat, C.; Piccioli, M. In *NMR and Biomolecular Structure*; Bertini, I., Molinari, H., Niccolai, N., Eds.; VCH: Weinheim, 1991; p 31.
(42) Bax, A.; Freeman, R.; Morris, G. *J. Magn. Reson.* **1981**, *42*, 164.
(43) Bertini, I.; Capozzi, F.; Luchinat, C.; Turano, P. *J. Magn. Reson.* **1991**, *95*, 244.
(44) Macura, S. R.; Ernst, R. R. *Mol. Phys.* **1980**, *40*, 95.
(45) Davis, D. G.; Bax, A. *J. Am. Chem. Soc.* **1985**, *107*, 2820.
(46) Jenkins, B. J.; Lauffer, R. B. *Inorg. Chem.* **1988**, *27*, 4730–4738.

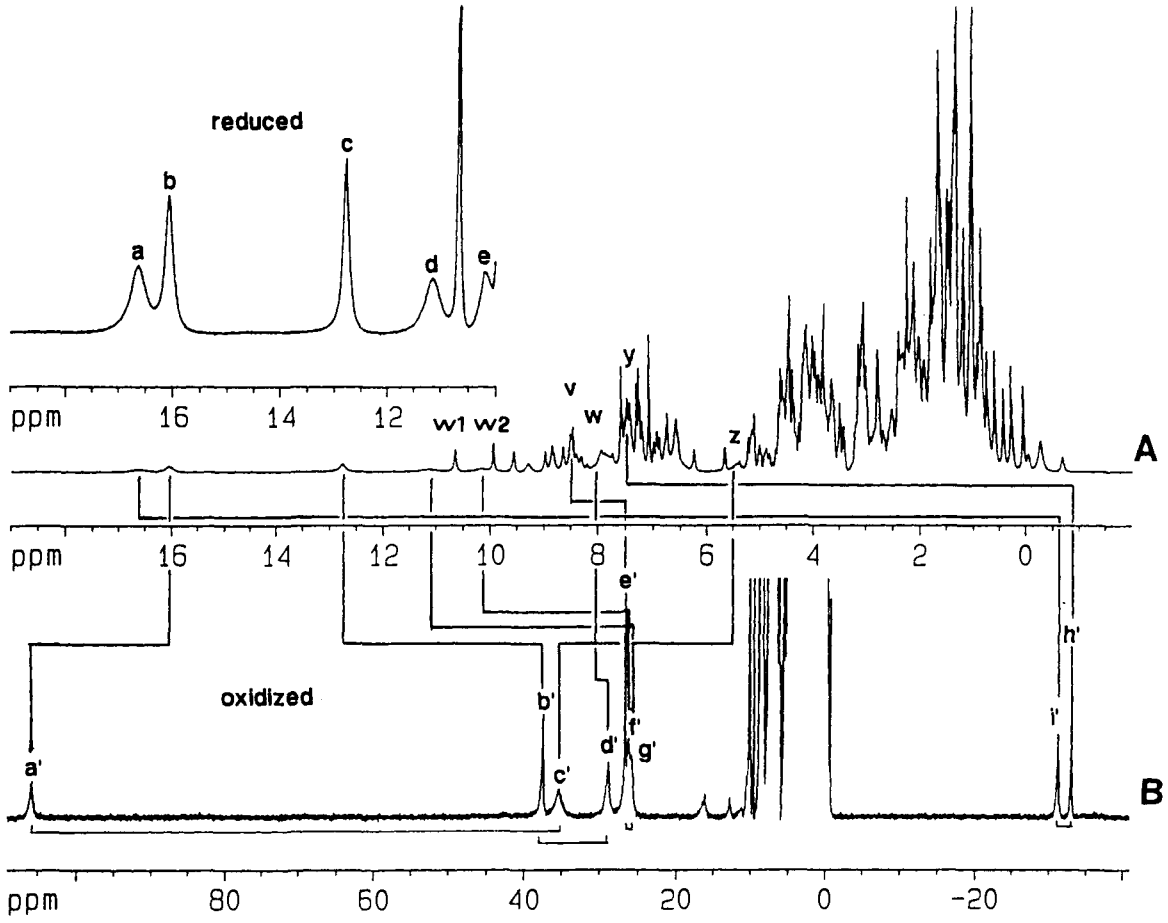

Figure 2. 600-MHz 300 K ^{1}H NMR spectra of HiPIP from *C. vinosum* in D_2O solutions, 50 mM phosphate buffer, recorded in the reduced (A), pH = 7.2, and oxidized state (B), pH = 5.4. Connectivities already established through EXSY experiments are drawn (ref 13). The geminal connectivities of the oxidized species are also indicated.

β-CH_2 or α-CH protons lie very close to protons belonging to the aromatic rings surrounding the cluster (Figure 6). The protons of the same residues in the oxidized protein can also be identified through the same procedure or through EXSY experiments. We thought that in spite of the fast nuclear relaxation rates these interproton distances could be short enough as to allow detection of ^{1}H NOE connectivities in monodimensional or bidimensional experiments. Indeed, careful inspection of the 1D NOE and 2D NOESY spectra of the protein in both oxidation states allowed detection of most of these short range connectivities from Cys protons to the aromatic protons; this led to the sequence-specific assignment of all the Cys residues, as described below. The observation of connectivities between the aromatic protons and the β-CH_2 protons of the cysteines bound to the cluster confirms the previous assignment.

Sequence-Specific Assignment of Cluster Liganded Cysteines. (1) Assignment of Cys II as Cys 46. By inspection of Figure 5 we note that signal f′ gives NOE to a signal at 10.2 ppm. (It has to be noted that the signal observed in Figure 5 at 10.2 ppm is actually the sum of a broad component, corresponding to saturation transfer from signal f′ to signal e, which arises from $\simeq$10% of the reduced form, and of a narrow component corresponding to the effective NOE.) Careful inspection of the 1D spectrum shows that in the region around 10.2 ppm there are three relatively sharp signals, two of which accidentally coincident at 10.22 ppm and the third, partially resolved, at 10.14 ppm. With an increase in temperature, the two coincident signals at 10.22 ppm start to be resolved. An EXSY experiment at 303 K (Figure 7) shows that the two signals (now at 10.24 and 10.21 ppm) give saturation transfer with signals at 10.65 (w1) and 9.94 ppm (w2), respectively. The chemical shift of the latter two signals suggests that they belong to Trp ring NH protons. These signals indeed show a progressive decrease in intensity, in D_2O samples, over a period of months. The TOCSY spectrum in the aromatic region (Figure 8C) clearly shows the full spin pattern of two Trp residues. The NOESY cross peaks (Figure 8A) identify signals w1 and w2 as the respective ring NH protons.

Chromatium vinosum HiPIP contains three Trp residues, one of which (Trp 60) on the surface of the protein and two (Trp 76 and Trp 80) in the vicinity of the cluster. The very slow exchange rate of signals w1 and w2 suggests that they belong to the latter two residues. Of the two, Trp 80 has the five-membered ring closer to the cluster, whereas the reverse is true for Trp 76. On the basis of the pattern of the T_1 values, we can tentatively assign w1 as belonging to Trp 80 and w2 as belonging to Trp 76.

From the X-ray data[47] (Figure 6), it appears that the ring NH proton of Trp 80 is actually close enough to a cysteine β-CH_2 proton (2.9 Å from Hβ1 of Cys 46) to give rise to a dipolar connectivity. Given the uniqueness of this feature, observation of the above NOE in the oxidized species from f′ to 10.22 ppm unequivocally identifies signal f′ as the Hβ1 of Cys 46 and confirms the assignment of w1 to Trp 80. As a consequence, signal g′ is assigned as the Hβ2 proton of the same cysteine (cysteine II) and signals d and e to the Hβ2 and Hβ1 of Cys 46 in the reduced form.

The observation of a COSY cross peak between signal d and its α-CH proton at 4.3 ppm (Figure 3A) and of a NOESY cross peak between signal e and the same signal (Figure 3B) is consistent with the β-CH/α-CH distances and dihedral angles in Cys 46 (Table I). The farther β-CH/α-CH pair forming a dihedral angle of 166° is expected to have stronger scalar coupling, according to the well-known dependence of J on the squared cosine of the dihedral angle.[48]

(47) (a) Carter, C. W., Jr.; Kraut, J.; Freer, S. T.; Xuong, Ng H.; Alden, R. A.; Bartsch, R. G. *J. Biol. Chem.* **1974**, *249*, 4212. (b) Carter, C. W.; Kraut, J.; Freer, S. T.; Alden, R. A. *J. Biol. Chem.* **1974**, *249*, 6339.

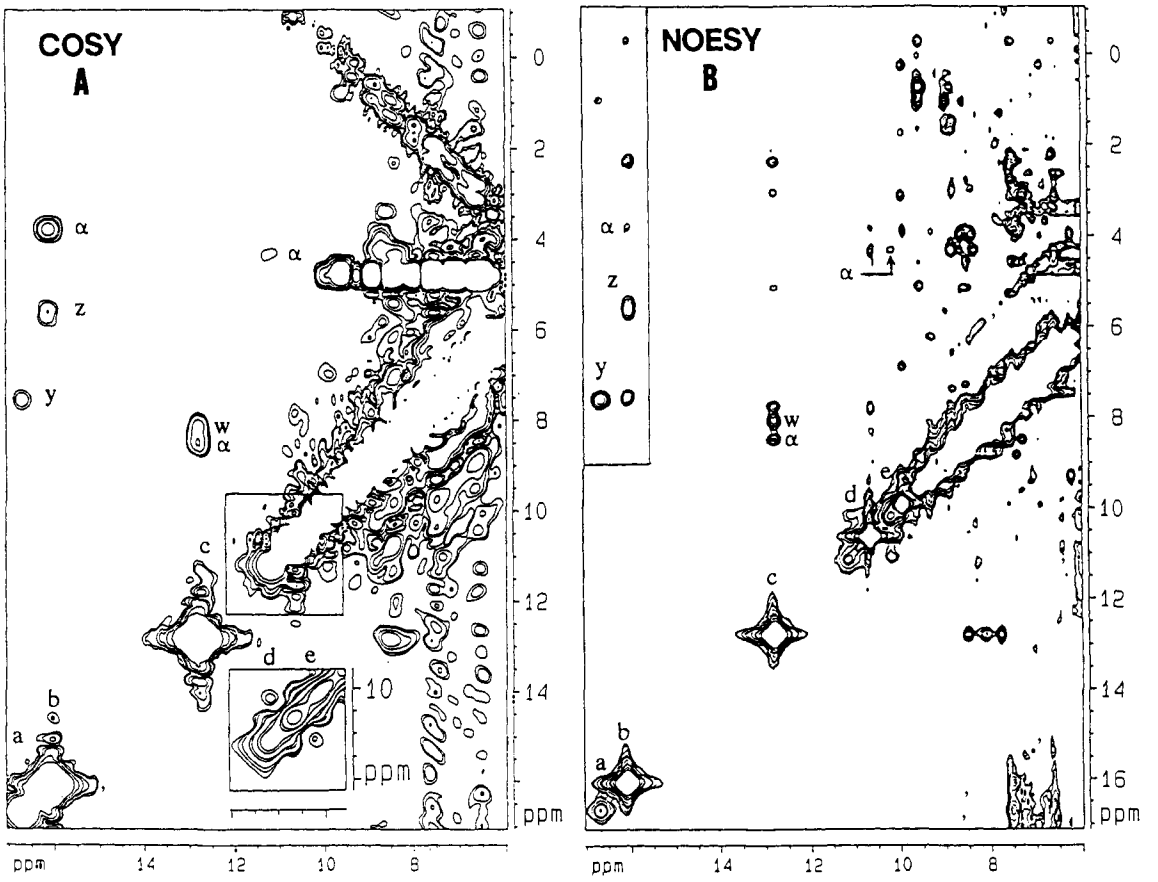

Figure 3. 600-MHz 300 K ^{1}H NMR COSY (A) and NOESY (B) spectra of reduced *C. vinosum* HiPIP. Conditions: COSY spectrum, magnitude mode, 512 data points in f_2 and 256 data points in f_1, zero filled to 1K × 1K, squared sine bell weighting function applied in both dimensions. The inset in the lower part of the figure shows the region between 10 and 12 ppm processed by application of a Gaussian weighting function (GB = 0.07; LB = −220 Hz over 1K data points in f_2 and 512 data points in f_1). NOESY spectrum, phase sensitive mode (TPPI), 512 data points in f_2 and f_1, zero filled to 1K × 1K. Mixing time of 10 ms. A cosine bell weighting function was applied along both dimensions. The inset shows the region 15.5–17 ppm of the same NOESY spectrum but processed using 512 data points in f_2 and 384 data points in f_1 and a shifted squared sine bell weighting function along both dimensions.

Further experiments, aimed at finding connectivities within the oxidized and, separately, the reduced form, have been performed and found consistent with the above assignment. In particular, dipolar connectivities have been observed in the oxidized species between the signals of the NH and the Hδ1 protons of Trp 80, and between signal f′ and the signal of the Hδ1 proton of Trp 80.

(2) Assignment of Cys IV as Cys 77. Signal e′ in the oxidized form, assigned as α-CH proton of Cys IV, gives a sizable NOE to a signal in the aromatic region at 7.24 ppm and a weaker NOE to a signal at 6.98 ppm (Figure 5). From the NOESY spectrum of Figure 8B two cross peaks are apparent between the signal at 8.52 ppm, corresponding to signal e′ in the oxidized form, and two signals in the aromatic region, at 6.94 and 7.26 ppm, respectively. The latter two signals belong to the six-membered ring of Trp 76 (see Figure 8C).

Inspection of the X-ray structure[47] (Figure 6) shows that the α-CH proton of Cys 77 is at 2.8 Å from the Hε3 of Trp 76 and at 3.5 Å from the Hζ3 proton of Trp 76. Thus, also the assignment of Trp 76 is further confirmed. These data unequivocally assign signal e′ in the oxidized species (and thus the signal at 8.52 ppm in the reduced species) as the α proton of Cys 77. Signals b′ and d′ in the oxidized form and signals c and w in the reduced form are assigned as the respective β-CH_2 protons.

The individual assignments of the β-CH_2 protons can be made by analyzing the relative intensities of NOEs from signals b′ (9%) and d′(4%) to signal e′. In addition, it can be observed that signal d′ gives rise to an intense NOE to a signal at 6.8 ppm (Figure 5), which is likely to correspond to a Hδ ring proton of the nearby Tyr 19. From these observations it emerges that signal d′ has to be assigned to Hβ2 of Cys 77.

(3) Assignment of Cys III as Cys 63. Inspection of the X-ray structure[47] (Figure 6) shows that one β-CH_2 proton of Cys 63 lies very close to the Hδ2 ring proton of Phe 66 (the distance is 2.0 Å). The NOESY map of the reduced protein (Figure 3B) shows a connectivity between signal b and a signal at 7.52 ppm. Interestingly the latter signal corresponds to one of the three positions of the scalar spin pattern typical of a Phe residue (Figure 8D). Again, such connectivity between a β-CH_2 proton and a Phe ring proton is a unique feature; as a consequence we assign signal b as the Hβ2 of Cys 63 and the signal at 7.52 ppm as the Hδ2 proton of Phe 66. As an internal check of this assignment, it can be observed that both signal b and the signal at 7.52 ppm give an intense NOESY cross peak to a signal located at 2.40 ppm which should correspond to the spatially close Hβ2 of Phe 66; indeed, the latter is at 2.4 Å from the Hδ2 of Phe 66 and at 1.75 Å from Hβ2 of Cys 63.

On the basis of the above assignment, signals b and z in the reduced form and a′ and c′ in the oxidized form are respectively assigned as Hβ2 and Hβ1 of Cys 63.

(4) Assignment of Cys I as Cys 43. We are left with the last pair of signals (h′–i′ in the oxidized form and a–y in the reduced form) which, as a result of the previous assignments, have to correspond to the β-CH_2 protons of Cys 43. Interestingly, we observe that signal h′ gives rise to two intense NOE connectivities in a region typical of NH protons (at 10.1 and 8.70 ppm) (Figure 5). Inspection of the structure shows that the Hβ1 proton of Cys 43 lies very close to the NH protons of Cys 43 itself and of Ala 44. This allows us to assign signal h′ as a Hβ1 proton of Cys 43

(48) (a) Karplus, M. *J. Chem. Phys.* **1959**, *30*, 11. (b) Karplus, M. *J. Am. Chem. Soc.* **1963**, *85*, 2870.

Table I. Sequence Specific Assignments of the Cysteine Protons in the Oxidized and Reducted State of *C. vinosum* HiPIP[a]

		δ, ppm (300 K)						
		reduced (pH* = 7.2)		oxidized (pH* = 5.4)				
residue						Fe–H, Å	β–α, Å	β–C–C–α dihedral angles, deg
cysteine 43	β1	y	7.57	h′	−31.20	4.02	3.00	174.8
	β2	a	16.7	i′	−33.01	2.96	2.45	−67.6
	α					2.99		
cysteine 46	β1	e	10.16	f′	26.41	3.44	2.29	47.6
	β2	d	11.13	g′	25.91	3.09	2.97	166.0
	α		4.3			4.99		
cysteine 63	β1	z	5.52	c′	35.32	3.17	2.52	63.7
	β2	b	16.10	a′	105.82	3.99	3.06	−177.1
	α		3.75			4.42		
cysteine 77	β1	c	12.77	b′	37.57	4.12	2.20	−35.2
	β2	w	8.06	d′	28.90	3.08	2.51	81.4
	α	v	8.52	e′	26.75	4.97		

[a] Metal to proton distances, β–α interproton distances, and H–Cβ–Cα–H dihedral angles, taken from the X-ray structure of the oxidized form (ref 47), are reported.

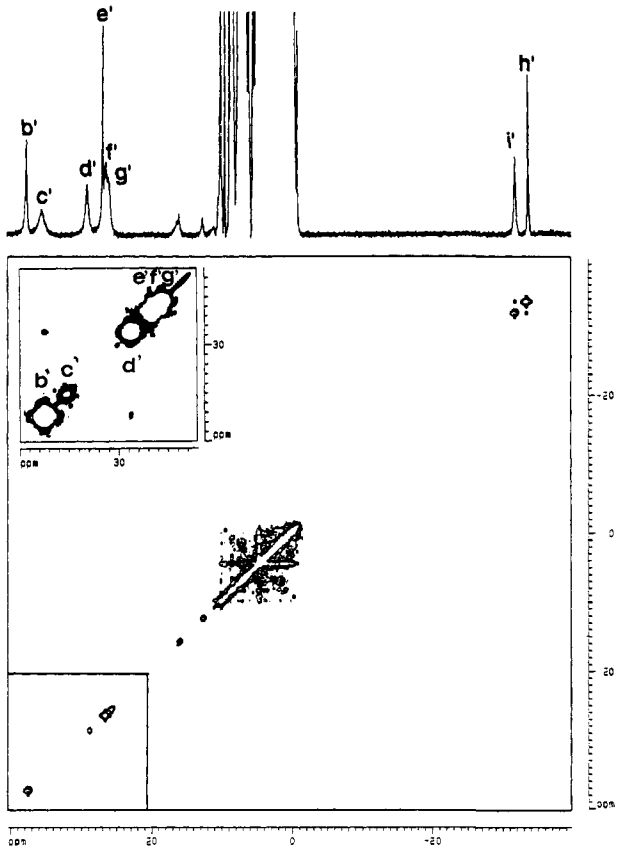

Figure 4. 600-MHz 300 K ^{1}H NMR COSY spectrum of oxidized *C. vinosum* HiPIP. The inset shows a different processing for the 40–25 ppm region. Conditions: magnitude mode, 2K data points in f_2, 1K data points in f_1, zero filled to 2K × 2K. Inset: 1K data points in f_2, 512 points in f_1, zero filled to 2K × 2K. A squared sine bell weighting function was used in both cases.

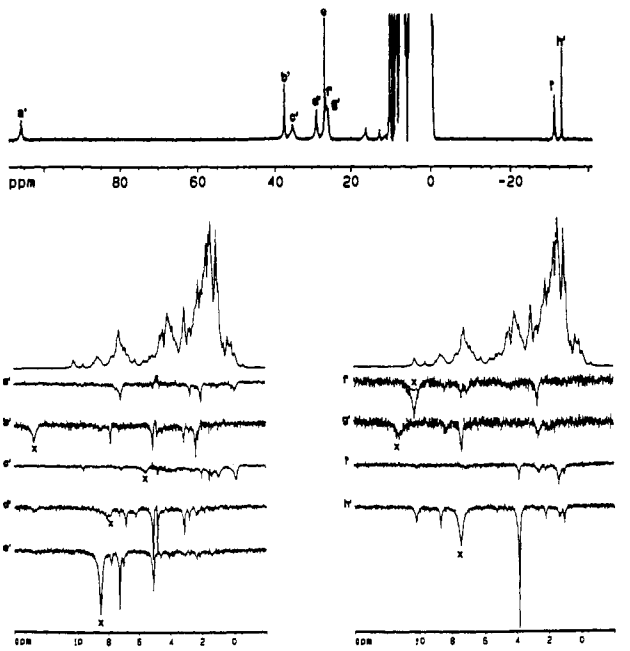

Figure 5. 600-MHz 300 K ^{1}H NMR NOE difference spectra of oxidized *C. vinosum* HiPIP obtained upon saturation of each of the β-CH_2 proton resonances and of one α-CH proton in the oxidized state. The difference spectra are labeled according to which signal is saturated. The saturation time was 80 ms for all signals. Signals labeled with × are saturation transfer effects to the corresponding protons in the reduced form, which is present at ≃10%. The different spectra are scaled in such a way that the areas of the irradiated signals (spectrum shown in the upper part of the figure) are all equal.

and to state that the above mentioned NH protons are unexchanged in D_2O.

It is worth noting here that, in the oxidized protein, signal i′ gives a NOE to a broad signal located at 2.60 ppm, which, in turn, is dipolar coupled to signal g′, Hβ2 of Cys 46 (Figure 5). From analysis of the structural data, it follows that the broad signal at 2.60 ppm is likely to correspond to the α-CH proton of Cys 43. These observations complete the sequence-specific assignment of the β-CH_2 protons of the cluster-bound cysteines.

As it appears from Table I, not all the α-CH protons have been unequivocally identified because not all the scalar connectivities with β-CH_2 protons have been detected and more than one dipolar connectivities with β-CH_2 protons have been observed for each cysteine (see for example Figure 5).

Internal Consistency of the Assignment: COSY and NOESY Complementarity. The correctness of the assignment may be further confirmed by analyzing the NOESY and COSY connectivities of the Cys β-CH_2 protons to the respective α-CH protons and establishing whether the observed ones correspond to those which, on the basis of structural data, are expected to be the more intense. The H–$C_β$–$C_α$–H dihedral angle influences the value of the $H_α$–$H_β$ coupling constant through a squared cosine relationship[48] and of the $H_α$–$H_β$ dipolar interaction which depends on the reciprocal of the sixth power of the interproton distance.[49] So, from inspection of Table I, we expect the largest values of *J* coupling constants (hence intense COSY cross peaks) for the following signal pairs: y–α, d–α, and b–α. The shortest interproton distances (hence intense NOESY cross peaks) are found for signal pairs: a–α, e–α, z–α, and c–α.

(49) Neuhaus, D.; Williamson, M. *The Nuclear Overhauser Effect in Structural and Conformational Analysis*; VCH Publications: New York, 1989.

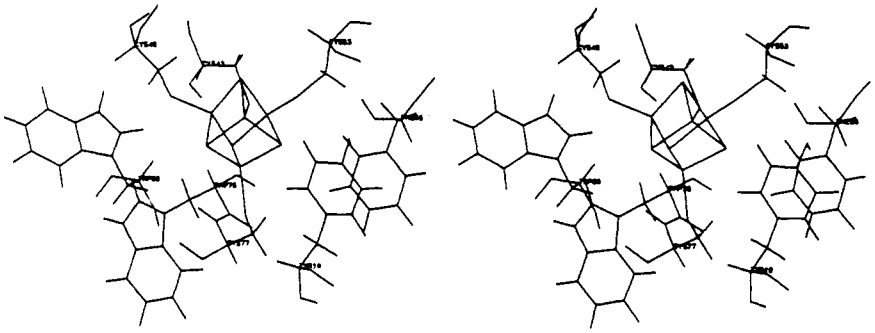

Figure 6. Stereoview of the cluster region of oxidized *C. vinosum* HiPIP (ref 47).

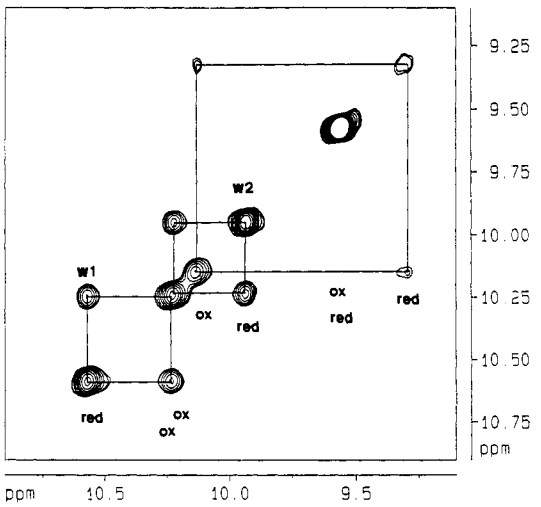

Figure 7. 600-MHz 303 K EXSY spectrum of a sample containing comparable amounts of oxidized and reduced *C. vinosum* HiPIP at pH 5.3. Detail of the region where Trp NY proton resonances are expected to fall.

Despite the fact that the intensity of the COSY and NOESY cross peaks is modulated by the nuclear relaxation times of the connected signals, we observe that the above expectations are fulfilled, at least in a qualitative way, by the experimental results, in excellent agreement with our assignment.

Further Assignments. Once the sequence-specific assignment of the cluster coordinated cysteines is achieved, it is possible to extend sequence-specific assignments to other residues which lie close to the assigned ones. For instance, we propose that the signal at 5.05 ppm in the spectrum of oxidized HiPIP, which is dipolarly connected to signals b′, d′ and e′ (Figure 5), is to be assigned to the α-CH proton of Tyr 19. The intense NOE observed on a signal at 3.8 ppm (Figure 5) upon irradiation of signal h′ suggests that the former signal has to be assigned to the spatially close α-CH of Val 73.

Signal a in the reduced protein gives a NOESY cross peak with a signal at 1.0 ppm (Figure 3B), which is likely to be assigned to the δ-CH_3 of Ile 71. On the other hand signal b is dipolarly connected to a methyl signal at −0.3 ppm, assigned to the γ-CH_3 of the same Ile residue.

Discussion

Assignments and the Theoretical Model. Implications. The above presented approach allowed us to perform, for the first time, sequence-specific assignments of cluster-coordinated cysteines in a Fe_4S_4 protein. Table I summarizes the assignments obtained here. The availability of these assignments, together with the recent rationalization of the hyperfine shifts in oxidized HIPIPs on theoretical grounds,[9-17] allows us to discriminate between the two iron ions with pure ferric character and the two iron ions constituting the mixed valence pair in the oxidized form. In the $S = {}^1/_2$ electronic ground state of the cluster the first pair has a subspin S smaller than the latter,[27] possibly $S = 4$ and $S = {}^9/_2$, respectively.[5] In the presence of antiferromagnetic coupling between the two pairs, the mixed valence pair with the larger S aligns with the magnetic field, whereas the $S = 4$ pair is opposite to the field. This does not occur for the excited states, characterized by total S values larger than ${}^1/_2$. Since the ground-state population is sizably larger than that of the excited states for J values of the order of kT as in the present system, the protons of the cysteines coordinated to the ferric ions are thus shifted upfield, or, if downfield, tend to reach an upfield shift by decreasing temperature, therefore showing the so-called anti-Curie behavior.[9,13-15] The former behavior is shown by the pair of signals h′ and i′, the latter by the pair of signals f′ and g′. These signals now identify Cys 43 and Cys 46. Therefore, the iron ions coordinated to cysteines 43 and 46 are those which show a pure ferric character in the oxidized protein. Conversely, cysteines 63 and 77, whose β-CH_2 signals are a′–c′ and b′–d′, respectively, coordinate the iron ions which form the mixed valence pair.

In the simple model proposed by us,[9,13-15] the hyperfine shifts experienced by the β-CH_2 protons of Cys 63 and Cys 77 should be the same, as should be the shifts experienced by the other two cysteines. Obviously, in a real low-symmetry system like a protein, this is not the case. First of all, even if the hyperfine coupling constants of each of the two cysteines for the two iron ions within one pair were the same, an angular dependence is expected due to the different overlap of the s orbital of the methylene protons with the molecular orbitals with larger unpaired spin density (see later). Second, it has been shown that the equivalence between the two ferric ions can be easily removed by even small changes in one or more of the six exchange coupling constants characterizing the system.[15] Indeed, relatively small perturbations are capable of reproducing the actual pattern of the shifts of the ferric pair in *C. vinosum*, i.e. one pair upfield and one pair downfield with anti-Curie behavior.[13]

On the other hand, it is more difficult to conceive a reason for the inequivalence of the two iron ions in the mixed valence pair. Mössbauer data show that the extra electron is fully delocalized over the two centers and should make them equivalent, in the absence of other sources of asymmetry. If asymmetry is present, then the extra electron may be distributed unequally or, in VB language, the two limiting structures with the extra electron on one center or on the other center may not have the same weight in the resulting resonance hybrid.

This situation would result in one iron having somewhat more ferrous character than the other. According to the simple Heisenberg description of the system, the protons of the cysteine coordinated to the iron with more ferrous character should be less downfield shifted. In this case b′–d′ (i.e. Cys 77) should belong to the more ferrous site. As opposed to iron(III), iron(II) experiences a sizable magnetic anisotropy and therefore is expected to give rise to sizable pseudocontact shifts. Consistent with this analysis, Cys 77 is the only cysteine whose α-CH proton is remarkably shifted from the diamagnetic position in both reduced and oxidized forms.

Correlation of the M–S–C–H Dihedral Angles with the Hyperfine Shifts. In the case of aliphatic amines coordinated to paramagnetic metal ions the following relation was found to hold

$$\delta = A + B\cos^2\theta$$

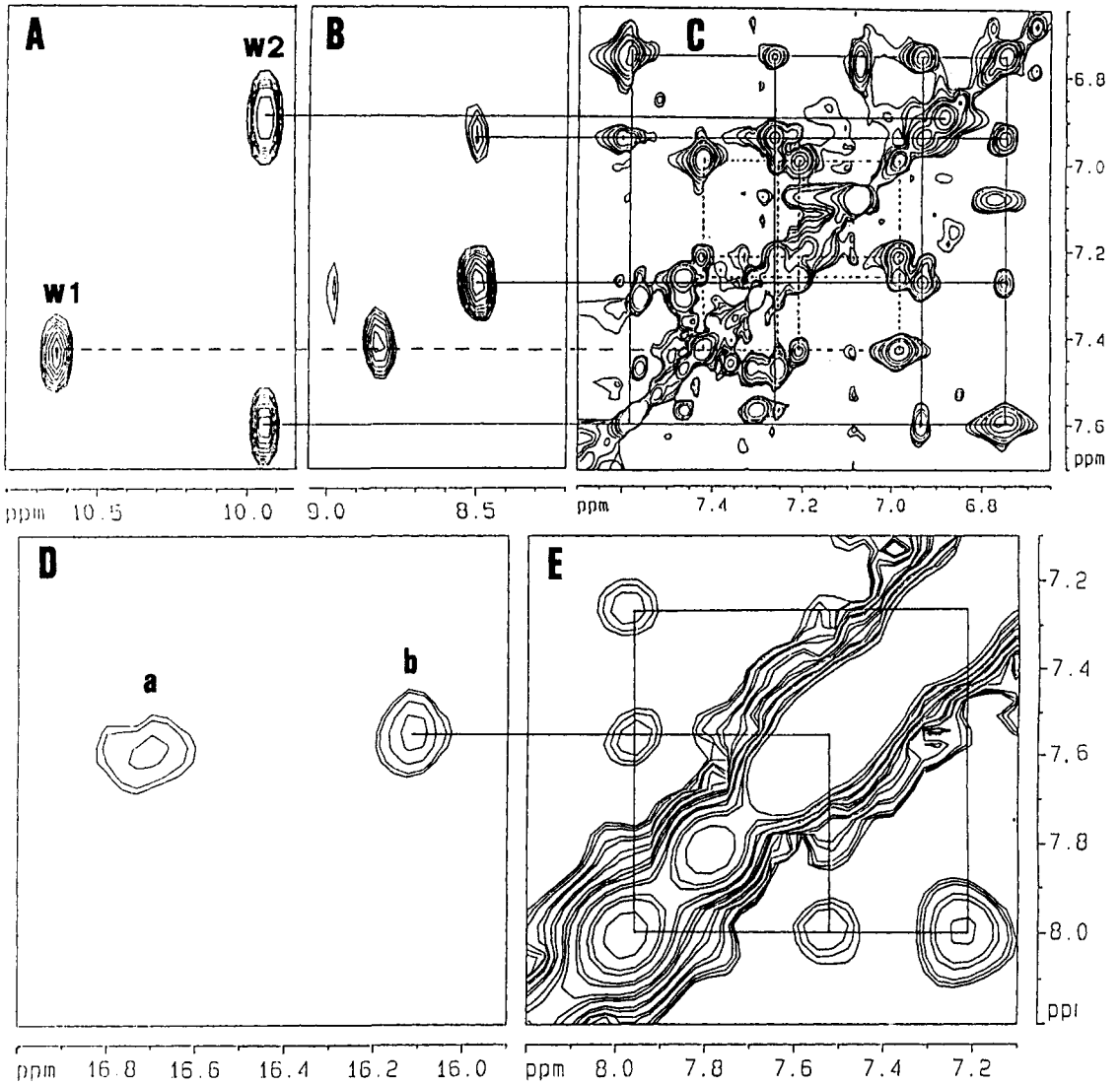

Figure 8. 600-MHz 300 K NOESY (A, B, and D), TOCSY (C), and COSY (E) spectra on the aromatic region of reduced *C. vinosum* HiPIP. The region of the TOCSY spectrum in which the spin system pattern of Trp residues occur is shown. The patterns of Trp 76 (——) and Trp 80 (– – –) are drawn. The COSY spectrum permits detection of the scalar pattern of Phe 66 (——). The NOESY spectrum allows detection of through-space connectivities from the Trp 80 and Trp 76 to the respective w1 and w2 NH protons (A), from Phe 66 to signal b (C), and from α-CH proton of Cys 77 and the Trp 76 Hϵ3 and Hζ3 protons (B) (see text). Conditions: TOCSY experiment, 2K × 1K data points, zero filled to 2K × 2K. Shifted squared sine bell functions were applied in both dimensions. Conditions for NOESY and COSY spectra have been reported above.

where θ is the M–N–C–H dihedral angle and $A \ll B$.[50-53] This empirical relationship is theoretically justified by assuming that most of the unpaired spin density, effective in inducing proton contact shifts, resides on the metal–nitrogen bond and that such a bond transfers spin density onto the methylene protons through a hyperconjugative mechanism.[50-53]

On the other hand, in CH moieties attached to carbon π radicals, the relevant dihedral angle must be defined relative to the carbon p orbital rather than to the σ orbitals of the sp^2 type.[54] In the case of cysteines coordinated to iron ions in a pseudotetrahedral symmetry both σ and π mechanisms could be operative, since unpaired electrons are present both in the σ antibonding t_2 orbitals and in the e orbitals which are able to form π bonding to the sulfur atom. In the former case a regular $\cos^2\theta$ dependence would be expected, whereas, if π overlap is very effective, a $\sin^2\theta$ dependence would be expected. $\cos^2\theta$ and $\sin^2\theta$ values are listed in Table II for both the oxidized and the reduced form. It is apparent that a $\cos^2\theta$ dependence is in striking disagreement with experimental data in both redox forms (Table I). A $\sin^2\theta$ dependence would be somewhat more consistent with the experimental data on the reduced form although the agreement is, at best, qualitative and only for cysteines 43, 46, and 63. Cysteine 77 could also be made consistent by assuming a decrease of about 10° of the dihedral angles with respect to the X-ray values. At this stage it is difficult to judge whether the discrepancies are due to the simplistic nature of the theory, to the neglect of sizable pseudocontact shifts, especially on the proton of each pair which is closer to the paramagnetic center, to inaccuracies of the X-ray derived dihedral angles, or to actual differences between solid-state and solution structures. The last hypothesis is considered unlikely

Table II. Hβ–C–S–Fe Dihedral Angles for Cys β-CH_2 Protons in Both Oxidized[47] and Reduced[55] States of HiPIP from *C. vinosum*

		reduced			oxidized		
		θ	$\sin^2\theta$	$\cos^2\theta$	θ	$\sin^2\theta$	$\cos^2\theta$
Cysteine 43	β1	173	0.01	0.99	165.4	0.06	0.94
	β2	53	0.64	0.36	45.4	0.51	0.49
Cysteine 46	β1	60	0.75	0.25	77.8	0.96	0.04
	β2	−60	0.75	0.25	−42.2	0.45	0.55
Cysteine 63	β1	3	0	1	8.0	0.02	0.98
	β2	−117	0.79	0.21	−112.0	0.86	0.14
Cysteine 77	β1	154	0.19	0.81	150.0	0.25	0.75
	β2	34	0.31	0.69	30.0	0.25	0.75

(50) Mc Connell, H. M. *Proc. Natl. Acad. Sci. U.S.A.* **1972**, *69*, 335.
(51) Pratt, L.; Smith, B. B. *Trans. Faraday Soc.* **1969**, *65*, 915.
(52) Ho, F. F.-L.; Reilley, C. N. *Anal. Chem.* **1969**, *41*, 1835.
(53) Fitzgerald, R. J.; Drago, R. S. *J. Am. Chem. Soc.* **1968**, *90*, 2523.
(54) Karplus, M.; Frankel, G. K. *J. Chem. Phys.* **1961**, *35*, 1312.

in view of the substantial agreement of the present COSY and NOESY data with the α–β dihedral angles. Also T_1 and T_2 values[13] of the β-CH_2 protons are all qualitatively consistent with the relative Fe–H distances. As more sequence-specific assignments and X-ray data will be available in the near future for other Fe_4S_4 proteins, these hypotheses can be tested.

The reported variations in dihedral angles between the reduced and oxidized forms range from 4° for Cys 77 to 5° for Cys 63 to 8° for Cys 43 to 18° for Cys 46.[47,55] Interestingly, the largest variations are observed for cysteines now assigned as ligands to the iron(III) pair in the oxidized form; this is the pair that is likely to take up the electron upon reduction, whereas the other pair has already a mixed valence character.

One feature worth noting, anyway, is that on passing from the reduced to the oxidized form, none of the cysteine β-CH_2 pairs maintains a same hyperfine coupling ratio. The change is not dramatic for cysteines 63 and 77, and still relatively small (although with an inversion between the more and the less shifted signal) for cysteine 46. On the contrary, Cys 43 is strikingly different. In the reduced form the two β-CH_2 signals a and y show a very large difference in hyperfine shifts, whereas in the oxidized form the corresponding h′ and i′ signals are almost coincident at room temperature. It is clear that some local structural change must occur upon oxidation. From the X-ray data the dihedral angles for Cys 43 do change by 8° upon oxidation.[47,55] The actual values are consistent with the reduced form but not with the oxidized form. Independently of the model for contact shift, a change of the dihedral angle of as much as 23° (i.e. 15° more than observed) would be needed to make the shifts equivalent as observed in the oxidized form. Also, it should be noted that the hyperfine shift slopes for the h′ and i′ signals with temperature are very different. In particular, by lowering the temperature, the shift of signal i′ increases much more in absolute value than that of signal h′. At very low temperature (outside the accessible range in water) the shift ratio would tend to be similar to that of the reduced form. This observation does not find justification in the magnetic coupling model but must be due to an additional phenomenon. The observation can be rationalized in terms of a fast equilibrium between two conformations, one similar to that found in the X-ray structure and the other with dihedral angles such that the shifts are reversed. The latter would become increasingly accessible in the oxidized form by increasing temperature. At room temperature this equilibrium would be close to 50/50. It is also interesting to note in this respect that the shifts of signals i′ and h′ at room temperature are reversed by increasing pH above $\simeq$7.[34]

Inferences for the Electron Transfer Mechanism. The X-ray structure shows that the Fe_4S_4 cluster in *C. vinosum* HiPIP is almost completely buried and inaccessible to solvent. It is known that electrons can travel fast over long distances in the interior of a protein provided that efficient pathways are present.[56] This could be the case for *C. vinosum* HiPIP as well. However, one edge of the cluster, constituted by a sulfide ion, is visible from outside the protein, in a rather hydrophobic region of the surface, which could be a van der Waals interaction site. This sulfide ion is the one bridging the iron ions coordinated by Cys 46, Cys 63, and Cys 77. The iron coordinated by Cys 43 is completely buried. In the case that this sulfide is part of the electron transfer pathway from an outside electron donor, we can easily envisage a transfer to the iron coordinated by Cys 46, which is one of the pure ferric ions. The electron would then be shared with Cys 43 forming a second mixed valence pair. Indeed, the Cys 43 resonances show the largest changes upon reduction.

(55) Carter, C. W. Private communication.
(56) Gray, H. B.; Malmstrom, B. G. *Biochemistry* **1989**, *28*, 7499.

Concluding Remarks

This research has shown that once the structure is known, the combined use of Mössbauer data, theoretical approaches, and ^1H NMR spectra may establish the location of the iron ions with their electron spin moments within the protein frame. In the case of oxidized *C. vinosum* HiPIP, one of the two iron(III) ions is deeply buried inside the protein. The second ferric ion and the mixed valence pair share a bridging sulfide which is partially exposed on a hydrophobic region of the surface. The iron(III) ion is bound to Cys 46, and the mixed valence pair is bound to Cys 63 and Cys 77. It is possible that the iron bound to Cys 77 has a more ferrous character. When the cluster is reduced, all the iron ions have an oxidation state of +2.5. A large differentiation in the hyperfine shifts of the geminal β-CH_2 protons occurs upon reduction for Cys 43, which is coordinated to iron(III) in the oxidized form. The decrease in oxidation number, which is linked to an increase of the ionic radius, may cause a conformational rearrangement of the ligand. Cys 43 may be more mobile also in the oxidized state, as suggested by the different slopes of the temperature dependence of the hyperfine shifts of the geminal protons and by the pH dependence of the shift.

The actual hyperfine shifts have been related to the conformation of the cysteines, through the X-ray structural data. It appears that the electron delocalizes both through σ and π iron–sulfur bonds, with a predominance of the latter. It follows that the dependence of the hyperfine shifts on the Fe–S–C–H dihedral angle θ is dominated by a $\sin^2\theta$ function.

This research shows that 2D NMR of paramagnetic molecules is now at a level that allows the observation of connectivities between signals whose T_1 values are of the order of a few milliseconds and line widths of the order of several hundreds of hertz. This represents a great step toward the elucidation of the solution structure of paramagnetic metal sites in proteins by NMR.

Acknowledgment. Thanks are expressed to Professor Heinz Ruterjans and to Mr. Oliver Ohlenschlager for the initial 2D NMR experiments on the aromatic region on the reduced protein which eventually proved helpful for the present work. Financial support by C.N.R., Progetto Finalizzato Biotecnologie e Biostrumentazione is gratefully acknowledged.

Registry No. Cys, 52-90-4.